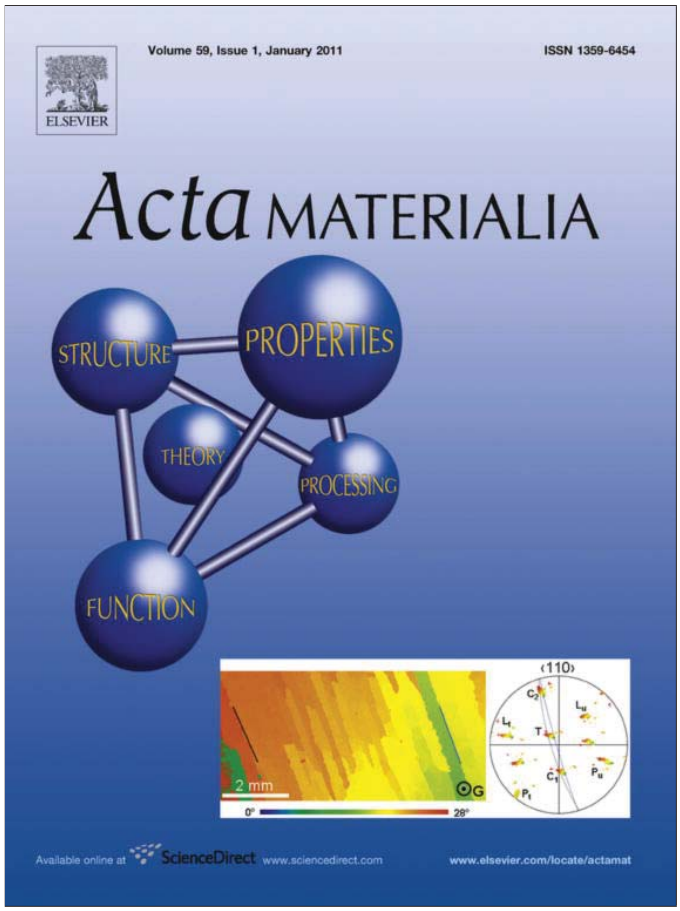

(This is a sample cover image for this issue. The actual cover is not yet available at this time.)

Report Documentation Page

Form Approved
OMB No. 0704-0188

1. REPORT DATE	2. REPORT TYPE	3. DATES COVERED
2011		**00-00-2011 to 00-00-2011**

4. TITLE AND SUBTITLE	5a. CONTRACT NUMBER
Calculations of intersection cross-slip activation energies in fcc metals using nudged elastic band method	5b. GRANT NUMBER
	5c. PROGRAM ELEMENT NUMBER
6. AUTHOR(S)	5d. PROJECT NUMBER
	5e. TASK NUMBER
	5f. WORK UNIT NUMBER
7. PERFORMING ORGANIZATION NAME(S) AND ADDRESS(ES) **Johns Hopkins University,Department of Mechanical Engineering,Baltimore,MD,21218**	8. PERFORMING ORGANIZATION REPORT NUMBER
9. SPONSORING/MONITORING AGENCY NAME(S) AND ADDRESS(ES)	10. SPONSOR/MONITOR'S ACRONYM(S)
	11. SPONSOR/MONITOR'S REPORT NUMBER(S)

12. DISTRIBUTION/AVAILABILITY STATEMENT
Approved for public release; distribution unlimited

13. SUPPLEMENTARY NOTES

14. ABSTRACT

The nudged elastic band (NEB) method is used to evaluate activation energies for dislocation intersection cross-slip in face-centered cubic (fcc) nickel and copper, to extend our prior work which used an approximate method. In this work we also extend the study by including Hirth locks (HL) in addition to Lomer?Cottrell locks and glide locks (GL). Using atomistic (molecular statics) simulations with embedded atom potentials we evaluated the activation barrier for a dislocation to transform from fully residing on the glide plane to fully residing on the cross-slip plane when intersecting a 120 forest dislocation in both Ni and Cu. The initial separation between the screw and the intersecting dislocation on the (1 1 1) glide plane is varied to find a minimum in the activation energy. The NEB method gives energies that are 10% lower than those reported in our prior work. It is estimated that the activation energies for cross-slip from the fully glide plane state to the partially cross-slipped state at the 120 intersection forming GL in Ni and Cu are 0.47 and 0.65 eV respectively, and from the fully cross-slip plane state to the partially cross-slipped state forming LC are 0.68 and 0.67 eV. The activation energies for cross-slip from the fully glide plane state to the partially cross-slipped state at the 120 intersection forming HL in Ni and Cu are estimated to be 0.09 and 0.31 eV, respectively. These values are a factor of 3?20 lower than the activation energy for bulk cross-slip in Ni and, a factor of 2?6 lower than the activation energy for cross-slip in Cu estimated by Friedel?Escaig analysis. These results suggest that cross-slip should nucleate preferentially at selected screw dislocation intersections in fcc materials and the activation energies for such mechanisms are also a function of stacking fault energy.

15. SUBJECT TERMS

16. SECURITY CLASSIFICATION OF:			17. LIMITATION OF ABSTRACT	18. NUMBER OF PAGES	19a. NAME OF RESPONSIBLE PERSON
a. REPORT **unclassified**	b. ABSTRACT **unclassified**	c. THIS PAGE **unclassified**	**Same as Report (SAR)**	**11**	

Standard Form 298 (Rev. 8-98)
Prescribed by ANSI Std Z39-18

Available online at www.sciencedirect.com

SciVerse ScienceDirect

Acta Materialia 59 (2011) 7135–7144

Acta MATERIALIA

www.elsevier.com/locate/actamat

Calculations of intersection cross-slip activation energies in fcc metals using nudged elastic band method

S.I. Rao [a,*], D.M. Dimiduk [b], T.A. Parthasarathy [a], J. El-Awady [c], C. Woodward [b], M.D. Uchic [b]

[a] UES Inc., 4401 Dayton-Xenia Road, Dayton, OH 45432-1894, USA
[b] Air Force Research Laboratory, Materials and Manufacturing Directorate, AFRL/MLLM, Wright-Patterson AFB, OH 45433-7817, USA
[c] Department of Mechanical Engineering, Johns Hopkins University, Baltimore, MD 21218, USA

Received 5 July 2011; received in revised form 16 August 2011; accepted 19 August 2011

Abstract

The nudged elastic band (NEB) method is used to evaluate activation energies for dislocation intersection cross-slip in face-centered cubic (fcc) nickel and copper, to extend our prior work which used an approximate method. In this work we also extend the study by including Hirth locks (HL) in addition to Lomer–Cottrell locks and glide locks (GL). Using atomistic (molecular statics) simulations with embedded atom potentials we evaluated the activation barrier for a dislocation to transform from fully residing on the glide plane to fully residing on the cross-slip plane when intersecting a 120° forest dislocation in both Ni and Cu. The initial separation between the screw and the intersecting dislocation on the (1 1 1) glide plane is varied to find a minimum in the activation energy. The NEB method gives energies that are ~10% lower than those reported in our prior work. It is estimated that the activation energies for cross-slip from the fully glide plane state to the partially cross-slipped state at the 120° intersection forming GL in Ni and Cu are ~0.47 and ~0.65 eV, respectively, and from the fully cross-slip plane state to the partially cross-slipped state forming LC are ~0.68 and ~0.67 eV. The activation energies for cross-slip from the fully glide plane state to the partially cross-slipped state at the 120° intersection forming HL in Ni and Cu are estimated to be ~0.09 and ~0.31 eV, respectively. These values are a factor of 3–20 lower than the activation energy for bulk cross-slip in Ni and, a factor of 2–6 lower than the activation energy for cross-slip in Cu estimated by Friedel–Escaig analysis. These results suggest that cross-slip should nucleate preferentially at selected screw dislocation intersections in fcc materials and the activation energies for such mechanisms are also a function of stacking fault energy.

Keywords: Cross-slip; Activation energy; Nudged elastic band method; Nickel; Copper

1. Introduction

Cross-slip has been recognized as the single most important process underlying complex spatio-temporal developments in microstructure leading to dislocation multiplication, strain hardening, pattern formation and dynamic recovery [1,2]. Its kinetics determine several engineering properties of interest, including hardening rate, recovery, creep and fatigue. Physics-based modeling of these engineering properties requires a mechanistic understanding of cross-slip and suitable methods of translation of this understanding to higher level models. Towards such a goal, the importance of accurate calculations of cross-slip activation energy parameters was discussed in our recent work. Briefly, one requires quantitative estimates of cross-slip activation energies under internal stresses and barriers. Our approach has been to use atomistic simulations to gain insights into the cross-slip process and to calculate parameters that could be used to inform mesoscale simulations to accurately capture the atomic level physics of that dislocation process. Atomistic simulations predict relatively high energies for cross-slip in bulk via the

* Corresponding author. Tel.: +1 9372551318; fax: +1 9372553007.
E-mail address: satish.rao@wpafb.af.mil (S.I. Rao).

1359-6454/$36.00 © 2011 Acta Materialia Inc. Published by Elsevier Ltd. All rights reserved.
doi:10.1016/j.actamat.2011.08.029

Freidel–Escaig mechanism [3], wherein the locally cross-slipped screw dislocation immediately redissociates on the cross-slip plane. Thermal activation of the Freidel–Escaig mechanism would require substantial stress at temperatures where cross-slip is observed experimentally.

Previously, using atomistic (molecular statics) simulations with embedded atom potentials, we evaluated the activation barrier for a dislocation to transform from fully residing on the glide plane to fully residing on the cross-slip plane intersecting a 120° forest dislocation forming glide locks (GL) and Lomer–Cottrell locks (LCL) in both Ni and Cu [4,5]. These calculations used an approximate Escaig stress technique in the calculation procedure and while the errors were estimated to be small, they were not investigated. In the Escaig stress technique the activation energies were obtained by determining equilibrium configurations (energies) when variable pure tensile or compressive stresses are applied along the [1 1 1] direction on the partially cross-slipped state. In this work we use the better established nudged elastic band (NEB) method to determine the activation energies. We also extend our prior work to include Hirth locks (HL). In this work, the NEB method is used to evaluate the activation barrier for cross-slip at the 120° intersection forming three types of locks, GL, LCL and HL. The initial separation on the (1 1 1) glide plane between the screw and intersecting dislocation is varied to find a minimum in this activation energy. The screw dislocation under study had a ½[1 $\bar{1}$ 0] Burgers vector and the intersecting dislocation had either a ½[$\bar{1}$ 0 1] or a ½[$\bar{1}$ $\bar{1}$ 0] Burgers vector on the (1 $\bar{1}$ 1) plane and a 120° line orientation of [0 1 1]. Section 2 describes the simulation technique, the interatomic potentials used in the simulations and briefly the method used to depict and visualize the core structures. Finally, Section 3 presents the results of the simulations, Section 4 a brief discussion of the results and Section 5 gives a summary of the results.

2. Simulation technique

The atomistic simulations described here employed the three-dimensional (3-D) parallel molecular dynamics code LAMMPS [6], developed at Sandia National Laboratory. The simulation cell is a rectangular parallelepiped having the x-axis oriented along [1 $\bar{1}$ 0], the y-axis along [1 1 $\bar{2}$] and the z-axis along [1 1 1]. The dimensions of the simulation cell are 31.0 nm along the x-axis and 15.5 nm along both the y- and z-axes, corresponding to a simulation cell of ~670,000 atoms. Fixed boundary conditions were applied along all three directions with a region of ~1.25 nm thickness at the surfaces held fixed. The screw dislocation had a ½[$\bar{1}$ 1 0] Burgers vector and the 120° dislocation had a ½[$\bar{1}$ 0 1] or a ½[$\bar{1}$ $\bar{1}$ 0] Burgers vector and a [0 $\bar{1}$ $\bar{1}$] line direction. Initially the screw and intersecting dislocations were introduced into the cell using their anisotropic elasticity displacement fields. By varying the anisotropic displacement field for the screw dislocation through changes to the origin for the displacement field and relaxing using a conjugate gradient technique the fully glide plane and fully cross-slip plane core structures were obtained for the intersection. These two core structures for the intersection were obtained for four different initial separations of the screw and intersecting dislocations on the (1 1 1) glide plane, 0–7.35a_0 in steps of 2.45a_0. The relaxed fully glide plane and fully cross-slip plane core structures were taken as the initial and final states for the NEB calculations [7]. The NEB method was applied only to the inner atoms of the cell, atoms within $x = -7.5$ to +7.5 nm, y and $z = -4.5$ to +4.5 nm. A total of 16 replicates (including the initial and final states) were used in the NEB calculations, together with an inter-replica spring constant of 0.04 eV Å^{-2} [8]. Energy minimization for these calculations were performed using a damped dynamics technique for up to 20,000–80,000 fs [7]. The NEB calculations were used to determine the energy profile as the screw dislocation transformed from the fully glide plane state to the fully cross-slipped state. In all cases the energy profile showed a deep minimum approximately half-way between, corresponding to the partially cross-slipped state [4,5], and two activated maxima, one between the fully glide plane state and the partially cross-slipped state and one between the partially cross-slipped state and the fully cross-slipped state [5]. The energy difference between these activated states and the initial states (fully glide plane or fully cross-slipped states) gives the activation energy for cross-slip at the 120° intersections. The minimum in this activation energy for different initial separations of the screw and intersecting dislocations was taken to be the cross-slip activation energy at the 120° intersections for transforming the dislocation from the fully glide plane (GL1) to the partially cross-slipped state (PCS1), $\delta E_{\mathrm{GL1\text{-}PCS1}}$ (½[$\bar{1}$ 0 1] Burgers vector), or from the fully cross-slipped state (LC2) to the partially cross-slipped state (PCS1), $\delta E_{\mathrm{LC2\text{-}PCS1}}$ ([$\bar{1}$ 0 1] Burgers vector), or from the fully glide plane state (GL) to the partially cross-slipped state (PCSH), $\delta E_{\mathrm{GL\text{-}PCSH}}$ (½[$\bar{1}$ $\bar{1}$ 0] Burgers vector).

2.1. Potentials

The embedded atom potentials used for the simulations are those developed for face-centered cubic (fcc) Ni by Angelo et al. [9] based on the Voter and Chen format (Angelo), a Ni potential developed based on the Voter and Chen format which Rao et al. used within their Friedel–Escaig (FE) mechanism cross-slip simulations "vnih" [3], as well as a Ni potential developed by Mishin et al. [10]. The embedded atom potential used for simulations of Cu is that developed by Mishin et al. [11]. Table 1 gives the lattice parameter, cohesive energy, elastic constants and stacking fault energy for each of the potentials. The three Ni potentials used in the simulations give almost identical elastic constants, cohesive energies and lattice parameters (close to experimental values), whereas the stacking fault energy given by the potentials varies from 90 to 134 mJ m^{-2}. The Shockley partial spacing width d for the

Table 1
Lattice constant a_0, cohesive energy E_c, elastic constants C_{11}, C_{12} and C_{44}, stacking fault energy γ, and Shockley partial splitting of the screw dislocation d/b given by the three Ni potentials (Angelo, vnih and Mishin) and the Cu Mishin potential.

	Angelo (Ni)	vnih (Ni)	Mishin (Ni)	Mishin (Cu)
a_0 (Å)	3.52	3.52568	3.52	3.615
E_c (eV)	−4.45	−4.4346	−4.45	−3.54
C_{11} ($\times 10^{11}$ N m^{-2})	2.464	2.422	2.413	1.699
C_{12} ($\times 10^{11}$ N m^{-2})	1.473	1.472	1.508	1.226
C_{44} ($\times 10^{11}$ N m^{-2})	1.248	1.185	1.273	0.762
γ (mJ m^{-2})	89	119	134	44
d/b	6	4–5	4–5	6

screw dislocation varies from $d/b = 4$–5 for the vnih potential and Mishin potential to $d/b = 6$ for the Moody potential, where b is the magnitude of the Burger's vector of the screw dislocation. Since the experimentally determined stacking fault energy of Ni is close to 120 mJ m^{-2} the results of cross-slip activation energy for the vnih potential and Mishin potential should be representative of Ni. The embedded atom model (EAM) potential developed for Cu by Mishin et al. [11] gives a lattice parameter, cohesive energy, elastic constants and stacking fault energy which are very near experimental values and, cross-slip activation energy results from this potential should be representative of Cu. The Mishin potential gives a d/b ratio of 6 for Cu.

2.2. Depiction of core structures

In order to illustrate the relaxed screw dislocation geometries we take advantage of the increase in atomic energy produced by the strain field of the partial dislocations. By plotting the atoms having assigned energies within LAAMPs of greater than −4.42 or −4.40 eV (Ni) or −3.52 eV (Cu) (the energy of atoms in the stacking fault region) the Shockley partial dislocation cores can be easily imaged, even for these large simulation cells. In order to illustrate the cross-slipped segment products of the screw dislocation the positions are shown in a [1 1 1] as well as a [1 1 $\bar{2}$] projection (viewed directions). For the [1 1 $\bar{2}$] projection segments spread on the initial (1 1 1) plane appear as a single line and cross-slipped segments (i.e. on a (1 1 $\bar{1}$) plane) appear as a pair of partials separated by a stacking fault.

3. Results

3.1. Lomer–Cottrell locks and glide locks

Figs. 1 and 2 give the fully glide plane (GL1) and fully cross-slipped states (LC2) for the 120° intersection obtained using the Cu Mishin potential for initial separation distances of 0 and 4.90a_0. Figs. 1 and 2 show both the [1 1 1] and [1 1 $\bar{2}$] projections of the two core structures obtained for the intersection. Similar results were obtained for all three Ni potentials.

Figs. 3 and 4 give a plot of energy versus reaction coordinate obtained using the NEB method with the Cu Mishin potential for initial separation distances of 0 and 4.90a_0. A reaction coordinate of 0 corresponds to the fully glide plane state and a reaction coordinate of 1 corresponds to the fully cross-slipped state. In both cases the energy profile shows a deep minimum at a reaction coordinate of ∼0.4–0.5, which corresponds to the partially cross-slipped state [5]. The energy profile also shows two maxima, one at a reaction coordinate of ∼0.1–0.2 and the other at a reaction coordinate of ∼0.7–0.8. The energy difference between the activated maxima at a reaction coordinate of ∼0.1–0.2 and the fully glide plane state gives the activation energy for cross-slip from the fully glide plane state to the partially cross-slipped state $\delta E_{\text{GL1-PCS1}}$, and the energy difference between the activated maximum at a reaction coordinate of ∼0.7–0.8 and the fully cross-slipped state gives the activation energy for cross-slip from the fully cross-slipped state to the partially cross-slipped state, $\delta E_{\text{LC2-PCS1}}$, at the 120° intersection. The energies shown in Figs. 4 and 5 were measured for all the atoms in the cell (excluding the boundary atoms). The activation energy $\delta E_{\text{GL1-PCS1}}$ shows a minimum at an initial separation distance of 4.90a_0 between the screw and 120° intersecting dislocations, whereas $\delta E_{\text{LC2-PCS1}}$ shows a minimum at 0 separation distance. This behavior is most probably related to the details of the Escaig stress distribution from the 120° intersecting dislocation at the intersection. The activation energies $\delta E_{\text{GL1-PCS1}}$ and $\delta E_{\text{LC2-PCS1}}$ are measured to be 0.65 and 0.67 eV, respectively, with the Cu Mishin potential. Figs. 5 and 6 give plots of energy versus reaction coordinate obtained using the NEB method with the Ni Mishin potential for initial separation distances of 0 and 2.45a_0. Qualitatively, the Ni results are very similar to the Cu results, although the quantitative values of the activation energies and the energy minima change. The activation energies $\delta E_{\text{GL1-PCS1}}$ and $\delta E_{\text{LC2-PCS1}}$ are measured to be 0.47 and 0.68 eV, respectively, with the Ni Mishin potential.

Fig. 7 shows a plot of the activated states obtained using the NEB method with the Cu Mishin potential. The activated state for $\delta E_{\text{GL1-PCS1}}$ was obtained at an initial separation distance between the screw and intersecting dislocation of 4.90a_0, whereas the activated state corresponding to $\delta E_{\text{LC2-PCS1}}$ was obtained at 0 separation distance. For the activated state for transforming the screw dislocation from the fully glide plane state to the partially cross-slipped state a small portion of the screw dislocation at the intersection is on the (1 1 $\bar{1}$) cross-slip plane, whereas the rest of the screw dislocation is on the (1 1 1) glide plane. For the activated state for transforming the screw dislocation from the fully cross-slipped state to the partially cross-slipped state a small portion of the screw dislocation at the intersection is on the (1 1 1) glide plane, whereas the rest of the screw dislocation is on the (1 1 $\bar{1}$) cross-slip plane. The activation volume for cross-slip at the intersection with respect to the applied Escaig stresses can be estimated from the area of the activated region and is estimated to be

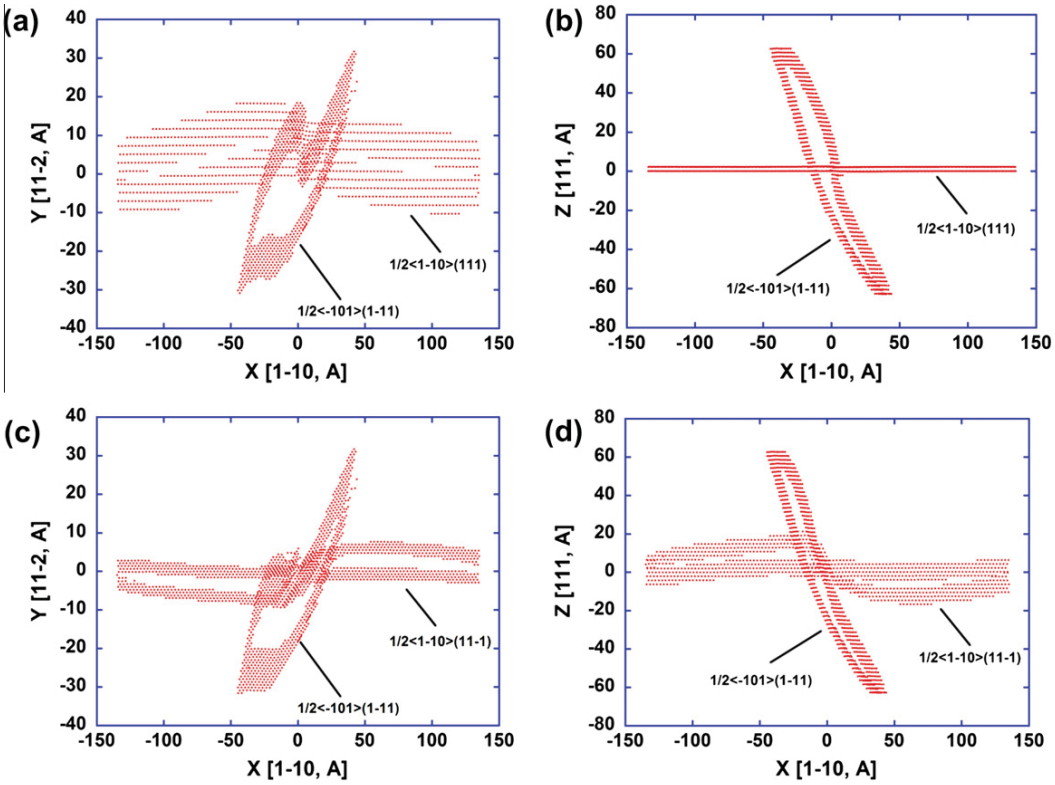

Fig. 1. The fully glide plane structure (GL1) obtained using the Cu Mishin potential shown in (a) the 1 1 1 and (b) the 1 1 $\bar{2}$ projections. The fully cross-slip plane structure (LC2) obtained using the Cu Mishin potential shown in (c) the 1 1 1 and (d) the 1 1 $\bar{2}$ projections. Both structures were obtained for an initial separation distance between the screw and intersecting dislocation of 0 on the (1 1 1) glide plane.

10–20b^3 in both cases. These results are very similar to previously obtained results for the structure of the activated states using the Escaig stress technique [5]. Fig. 8 shows a plot of the activated states obtained using the NEB method with the Ni Mishin potential. The activated state for $\delta E_{\text{GL1-PCS1}}$ was obtained at an initial separation distance between the screw and intersecting dislocation of 2.45a_0, whereas the activated state corresponding to $\delta E_{\text{LC2-PCS1}}$ was obtained at 0 separation distance. The activated structures are very similar to the ones obtained with the Cu Mishin potential.

Tables 2 and 3 give the activation energies for cross-slip at the 120° intersection, $\delta E_{\text{GL1-PCS1}}$ and $\delta E_{\text{LC2-PCS1}}$, obtained using the three different Ni potentials and the Cu Mishin potential as a function of the initial separation between the screw and intersecting dislocations (0–4.90a_0). For an initial separation of 7.35a_0 both $\delta E_{\text{GL1-PCS1}}$ and $\delta E_{\text{LC2-PCS1}}$ increased relative to the values at a separation of 4.90a_0 and, as a result, is not shown here. Tables 2 and 3 show that in all cases $\delta E_{\text{LC2-PCS1}}$ shows a minimum at 0 separation distance, whereas $\delta E_{\text{GL1-PCS1}}$ shows a minimum at a separation distance of 4.90a_0 for Cu and 2.45a_0 for Ni. The activation energy values for the Angelo, vnih and Cu Mishin potentials for a 0 separation distance are in fairly good agreement with previous calculations using the Escaig stress technique [5]. The Angelo potential gives anomalously low values for $\delta E_{\text{LC2-PCS1}}$. Considering the respective Mishin potentials to be representative of Ni and Cu and taking the minimum in activation energy as a function of the initial separation distance for both $\delta E_{\text{GL1-PCS1}}$ and $\delta E_{\text{LC2-PCS1}}$, the activation energies for cross-slip at this intersection are determined to be 0.47 and 0.68 eV for Ni and 0.65 and 0.67 eV for Cu. These values are a factor of 3–4 lower than the FE mechanism cross-slip activation energy for Ni (the Ni Mishin potential gives a value of 1.95 eV for the cross-slip activation energy using the FE mechanism) and a factor of 3 lower than the bulk cross-slip activation energy for Cu (the Cu Mishin potential gives a value of 1.7–1.8 eV for the cross-slip activation energy using the FE mechanism). The cross-slip activation energy values for Cu at the 120° intersection are in excellent agreement with the experimentally measured cross-slip activation energy of 0.61 eV for Cu [12]. These results suggest that cross-slip should preferentially nucleate at selected screw dislocation intersections in fcc materials.

3.2. Hirth locks

Fig. 9 gives the fully glide plane (GL) and fully cross-slipped states (CR) for the 120° intersection forming a HL obtained using the Cu Mishin potential for an initial separation distances of 0. Fig. 9 shows both the [1 1 1]

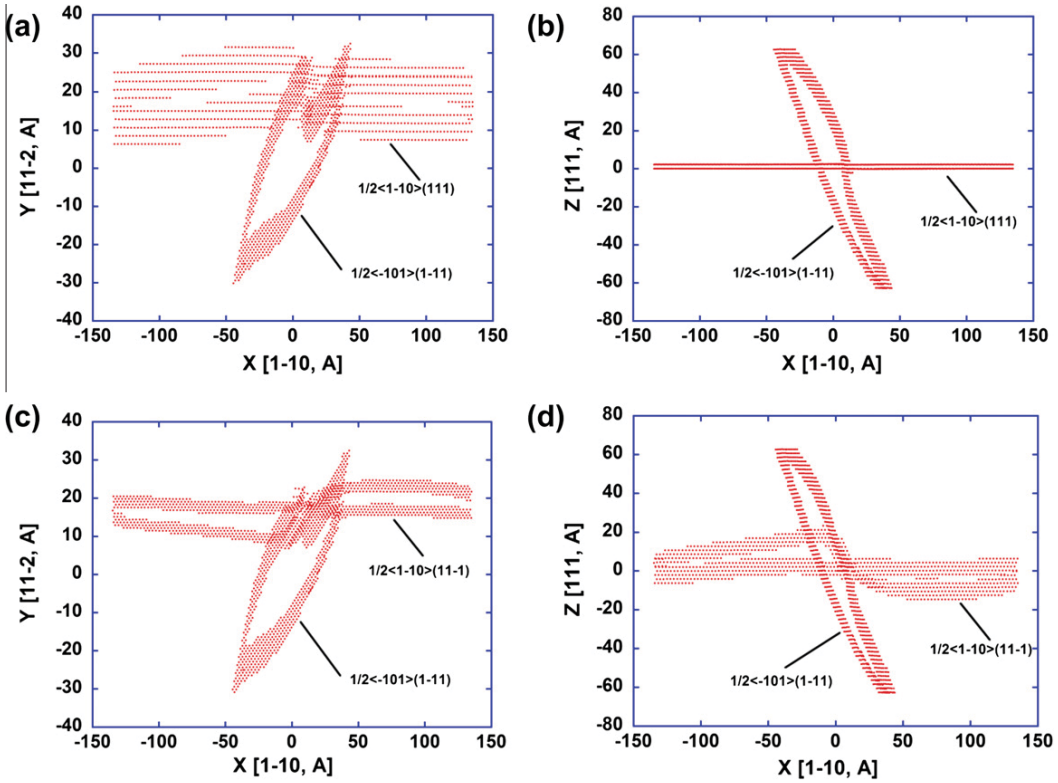

Fig. 2. The fully glide plane structure (GL1) obtained using the Cu Mishin potential shown in (a) the 1 1 1 and (b) the 1 1 $\bar{2}$ projections. The fully cross-slip plane structure (LC2) obtained using the Cu Mishin potential shown in (c) the 1 1 1 and (d) the 1 1 $\bar{2}$ projections. Both structures were obtained for an initial separation distance between the screw and intersecting dislocation of $4.90a_0$ on the (1 1 1) glide plane.

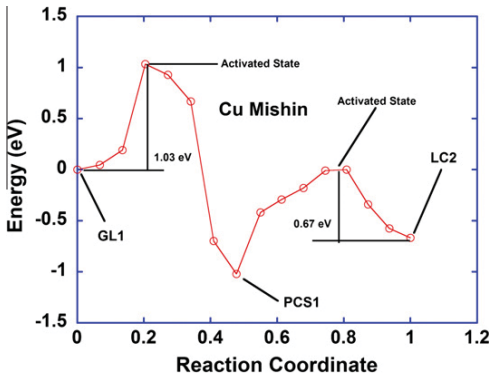

Fig. 3. Energy versus reaction coordinate obtained using the NEB method with the Cu Mishin potential at a 120° screw dislocation intersection. The initial separation distance between the screw and intersecting dislocation on the (1 1 1) glide plane was 0. A reaction coordinate of 0 corresponds to the fully glide plane state (GL1) and a reaction coordinate of 1 corresponds to the fully cross-slipped state (LC2).

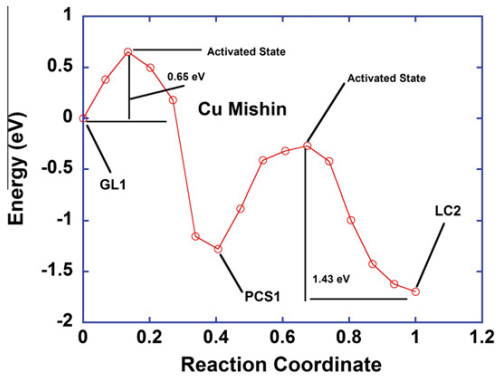

Fig. 4. Energy versus reaction coordinate obtained using the NEB method with the Cu Mishin potential at a 120° screw dislocation intersection. The initial separation distance between the screw and intersecting dislocation on the (1 1 1) glide plane was $4.90a_0$. A reaction coordinate of 0 corresponds to the fully glide plane state (GL1) and a reaction coordinate of 1 corresponds to the fully cross-slipped state (LC2).

and [1 1 $\bar{2}$] projections of the two core structures obtained for the intersection. Similar results were obtained for all other separation distances. Similar results were obtained with the Ni Mishin potential except for a separation distance of 0. For a separation distance of 0 the fully glide plane structure never materialized. To check that the fully glide plane structure is unstable at this intersection with the Ni Mishin potential the screw dislocation was initially introduced into the simulation cell as two Shockley partials separated by a distance of 4*b* on the (1 1 1) glide plane. Fig. 10a shows a plot of such initial conditions for the simulation in both the [1 1 1] and [1 1 $\bar{2}$] projections. When

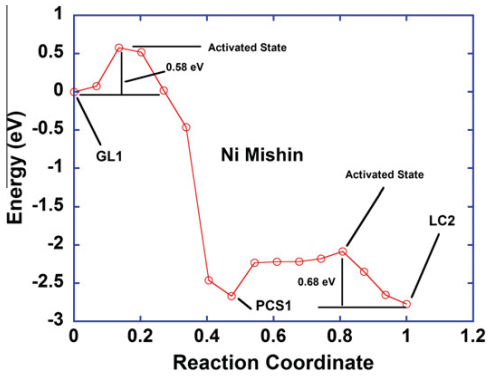

Fig. 5. Energy versus reaction coordinate obtained using the NEB method with the Ni Mishin potential at a 120° screw dislocation intersection. The initial separation distance between the screw and intersecting dislocation on the (1 1 1) glide plane was 0. A reaction coordinate of 0 corresponds to the fully glide plane state (GL1) and a reaction coordinate of 1 corresponds to the fully cross-slipped state (LC2).

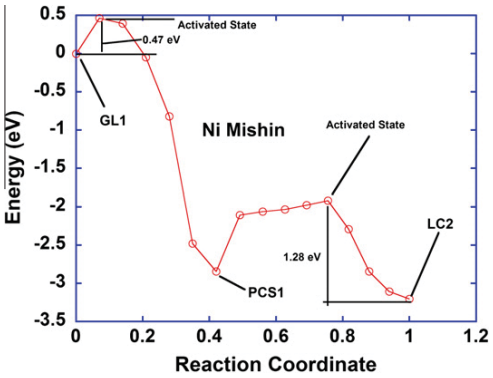

Fig. 6. Energy versus reaction coordinate obtained using the NEB method with the Ni Mishin potential at a 120° screw dislocation intersection. The initial separation distance between the screw and intersecting dislocation on the (1 1 1) glide plane was $2.45a_0$. A reaction coordinate of 0 corresponds to the fully glide plane state (GL1) and a reaction coordinate of 1 corresponds to the fully cross-slipped state (LC2).

relaxed the screw dislocation attains the configuration shown in Fig. 10b, where a small portion of the screw dislocation at the intersection spontaneously spreads on the cross-slip plane. This result suggests that the fully glide plane structure is unstable at this intersection for a 0 separation distance. The relaxed structure shown in Fig. 10b was taken as the initial state for the ensuing NEB calculations for this intersection corresponding to an initial separation distance of 0.

Fig. 11 gives a plot of energy versus reaction coordinate obtained using the NEB method with the Cu Mishin potential for an initial separation distance of 0. As before, the energy profile shows a deep minimum at a reaction coordinate of ~0.4–0.5, which corresponds to the partially cross-slipped state [4]. The energy profile also shows two maxima, one at a reaction coordinate of ~0.3–0.4 and the other at a reaction coordinate of ~0.4–0.7. The energy difference

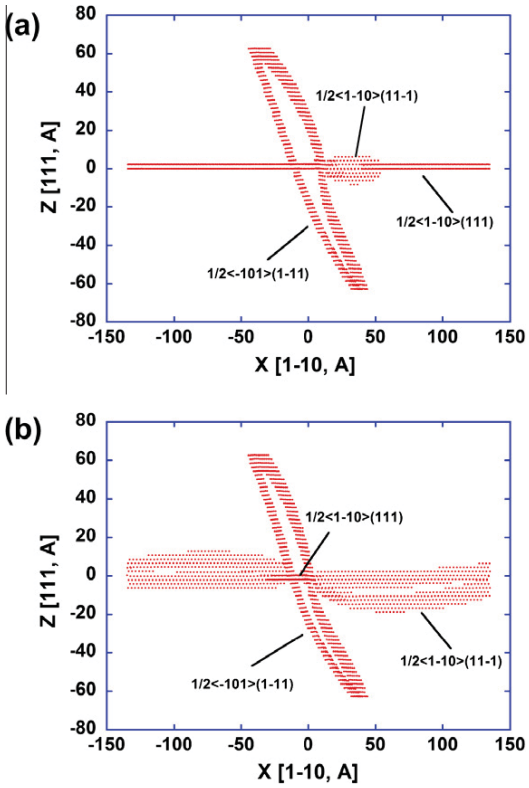

Fig. 7. A plot of the structure of the activated states for (a) transforming the dislocation from the fully glide plane state (GL1) to the partially cross-slipped state (PCS1) and (b) transforming the dislocation from the fully cross-slipped state (LC2) to the partially cross-slipped state (PCS1) obtained using the Cu Mishin potential. Both structures are shown in the $[1\,1\,\bar{2}]$ projection. (a) Result obtained for an initial separation distance between the screw and intersecting dislocations of $4.90a_0$ on the (1 1 1) glide plane; (b) result obtained for 0 separation distance.

between the activated maximum at a reaction coordinate of ~0.3–0.4 and the fully glide-plane state gives the activation energy for cross-slip from the fully glide plane state to the partially cross-slipped state $\delta E_{\text{GL-PCSH}}$ and the energy difference between the activated maximum at a reaction coordinate of ~0.4–0.7 and the fully cross-slipped state gives the activation energy for cross-slip from the fully cross-slipped state to the partially cross-slipped state $\delta E_{\text{CR-PCSH}}$ at the 120° intersection forming a HL. The activation energy $\delta E_{\text{GL-PCSH}}$ shows a minimum at an initial separation distance of 0 between the screw and 120° intersecting dislocations, whereas $\delta E_{\text{CR-PCSH}}$ is consistently large and will not be considered. The activation energy $\delta E_{\text{GL-PCSH}}$ is measured to be 0.31 and 0.44 eV with the Cu Mishin potential at initial separation distances of 0 and $2.45a_0$. The cross-slip activation energy values for Cu at the 120° intersection forming a HL are somewhat lower than the experimentally measured cross-slip activation energy of 0.61 eV for Cu [12]. Fig. 12 gives a plot of energy versus reaction coordinate obtained using the NEB method with the Ni Mishin potential for an initial separation distance of 0. Qualitatively, the Ni results are very similar to the Cu results,

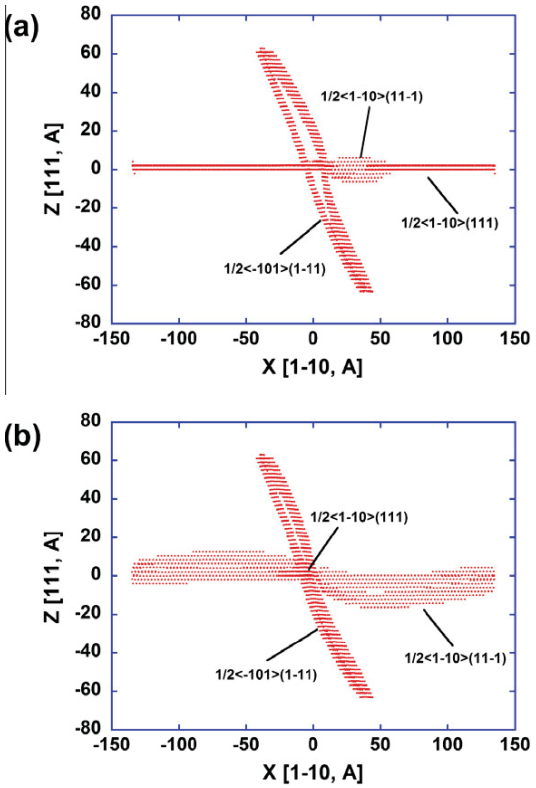

Fig. 8. A plot of the structure of the activated states for (a) transforming the dislocation from the fully glide plane state (GL1) to the partially cross-slipped state (PCS1) and (b) transforming the dislocation from the fully cross-slipped state (LC2) to the partially cross-slipped state (PCS1) obtained using the Ni Mishin potential. Both structures are shown in the $[1\,1\,\bar{2}]$ projection. (a) Result obtained for an initial separation distance between the screw and intersecting dislocations of $2.45a_0$ on the (1 1 1) glide plane; (b) result obtained for 0 separation distance.

Table 2
Activation energy for cross-slip from the fully glide plane state (GL1) to the partially cross-slipped state (PCS1) $\delta E_{\text{GL1-PCS1}}$ at the 120° intersection calculated using three different Ni potentials and the Cu Mishin potential as a function of the initial separation distance between the screw and intersecting dislocations on the (1 1 1) glide plane.

	0 (eV)	$2.45a_0$ (eV)	$4.90a_0$ (eV)
Angelo (Ni)	1.33	1.17	
vnih (Ni)	0.84	0.74	
Mishin (Ni)	0.58	0.47	0.58
Mishin (Cu)	1.03	0.73	0.65

Table 3
Activation energy for cross-slip from the fully cross-slipped state (LC2) to the partially cross-slipped state (PCS1) $\delta E_{\text{LC2-PCS1}}$ at the 120° intersection calculated using three different Ni potentials and the Cu Mishin potential as a function of the initial separation distance between the screw and intersecting dislocations on the (1 1 1) glide plane.

	0 (eV)	$2.45a_0$ (eV)	$4.90a_0$ (eV)
Angelo (Ni)	0.12	0.44	
vnih (Ni)	0.64	1.24	
Mishin (Ni)	0.68	1.28	
Mishin (Cu)	0.67	0.80	1.43

although the quantitative values of the activation energy and the energy minima change. The activation energy $\delta E_{\text{GL-PCSH}}$ is measured to be 0.09 and 0.16 eV with the Ni Mishin potential for initial separation distances of 0 and $2.45a_0$.

Fig. 13 shows a plot of the activated state ($\delta E_{\text{GL-PCSH}}$) obtained using the NEB method with the Cu Mishin potential for the 120° intersection forming the HL. The activated state was obtained for 0 initial separation distance between the screw and intersecting dislocation. For the activated state a significant portion of the screw dislocation at the intersection is on the $(1\,1\,\bar{1})$ cross-slip plane, whereas the rest of the screw dislocation is on the (1 1 1) glide plane. The activation volume for cross-slip at the intersection with respect to applied Escaig stresses can be estimated from the area of the activated region and is determined to be $\sim 60b^3$. Fig. 14 shows a plot of the activated state obtained using the NEB method with the Ni Mishin potential. As before, the activated state was obtained at an initial separation distance between the screw and intersecting dislocation of 0. The activated structure is very similar to the one obtained with the Cu Mishin potential, although it shows less spreading on the cross-slip plane and the activation volume for cross-slip with respect to applied Escaig stresses is estimated to be $20–30b^3$ with the Ni Mishin potential.

4. Discussion

In this work the NEB method was used to calculate the activation energy for cross-slip of screw dislocations at intersecting forest dislocations. Three different locking mechanisms were considered for the barrier mechanism, namely LCL, GL and HL. Two different fcc metals, Ni and Cu, with different stacking fault energies were considered. Several interesting observations can be made from the results. First, the activation energy for nucleation of cross-slip in an fcc metal can be sufficiently small to enable profuse cross-slip through thermal activation under multi-slip conditions. Second, the activation energy for GL and HL based cross-slip nucleation depends on the stacking fault energy, just as for the FE cross-slip mechanism. Third, the HL barrier offers the lowest barrier for cross-slip, which is only one-sixth of the FE mechanism value for copper and one-twentieth of the value for FE mechanism cross-slip in nickel.

The results clearly show that cross-slip nucleation at screw dislocations intersecting forest dislocations exhibits an activation energy that is a factor of 3–20 lower than that for the FE mechanism. It is worth noting that the probability of dislocation intersections is relatively large compared with other mechanisms of obstacle induced cross-slip, like cross-slip at screw dipoles, jogs and surfaces [13–15]. Further, cross-slip at screw dipoles, jogs and surfaces is athermal only under specific conditions [13–15]. The current results rationalize the experimentally observed profuse nature of cross-slip in fcc crystals in a more satisfactory manner than the current models of thermally activated cross-

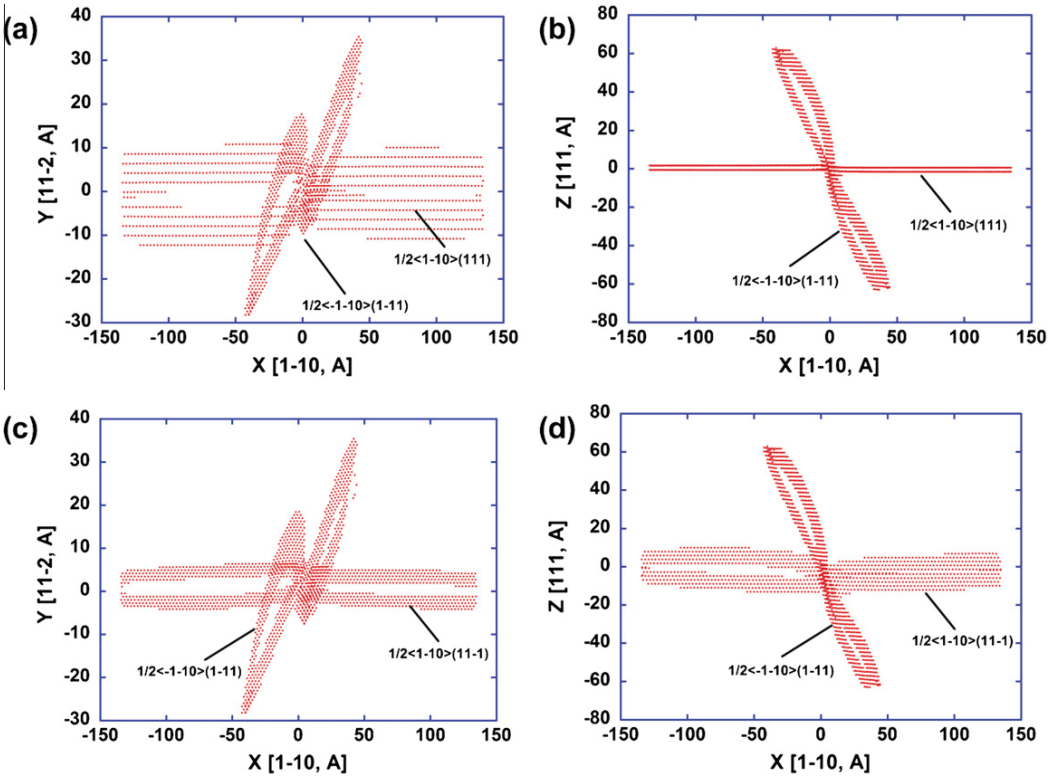

Fig. 9. The fully glide plane structure (GL) obtained at a 120° intersection forming a HL obtained using the Cu Mishin potential shown in (a) the 1 1 1 and (b) the 1 1 $\bar{2}$ projections. The fully cross-slip plane structure (CR) obtained using the Cu Mishin potential shown in (c) the 1 1 1 and (d) the 1 1 $\bar{2}$ projections. Both structures were obtained for an initial separation distance between the screw and intersecting dislocation of 0 on the (1 1 1) glide plane.

slip that require high stresses to provide a self-consistent explanation.

The new cross-slip nucleation mechanism has a variety of implications for crystal plasticity in fcc materials, as mentioned in our prior work, which is reiterated here. For example, within the present mechanism the frequency of cross-slip should scale with the forest dislocation density, i.e. a multiplication rate proportional to ρ_f. The growth of such nuclei should depend upon the relative magnitude of local stresses on the glide plane and the cross-slip plane at the partially cross-slipped screw–dislocation intersection region. Such behavior of the partially cross-slipped core under different modes of applied stress could be studied using atomistic simulations as well as dislocation dynamics simulations. Similar activation analysis using atomistic simulations must be performed for other intersections (varying the line direction of the intersecting dislocation) on the (1 $\bar{1}$ 1) plane that form GL, LCL or HL to determine the dependence of the activation energy for cross-slip on the line direction of the intersecting forest dislocation. The intersection mechanism of cross-slip nucleation should also be implemented in 3-D dislocation dynamics simulations as an alternative to the FE model for fcc materials.

According to Washburn [16], a double intersection cross-slip mechanism, where the segment that has been pulled into the cross-slip plane soon encounters another attractive intersection that brings it back onto another primary glide plane, provides a reasonable mechanism for dislocation multiplication and the growth of slip bands at low temperatures. Naturally such a mechanistic process must be demonstrated via modern simulation methods. Also, classical theories of strain hardening assume that dislocation storage in stage II of single crystal fcc materials is a result of junction formation [17] or two-dimensional (2-D) concave loop formation [18] as the gliding dislocation traverses through an array of forest dislocation obstacles on its glide plane. However, one of the major problems in classical strain hardening models is to explain how the generation of a 3-D network of stored dislocations occurs as a consequence of 2-D glide [18]. We note that the intersection cross-slip nucleation mechanism for dislocation storage may provide a convenient mechanism of generating a 3-D network of stored dislocations from 2-D glide.

5. Summary

NEB method calculations were conducted to identify the saddle point configuration and thus the activation energy for cross-slip of a screw dislocation in the presence of a 120° forest dislocation forming GL, LCL and HL. The initial separation between the screw and intersecting

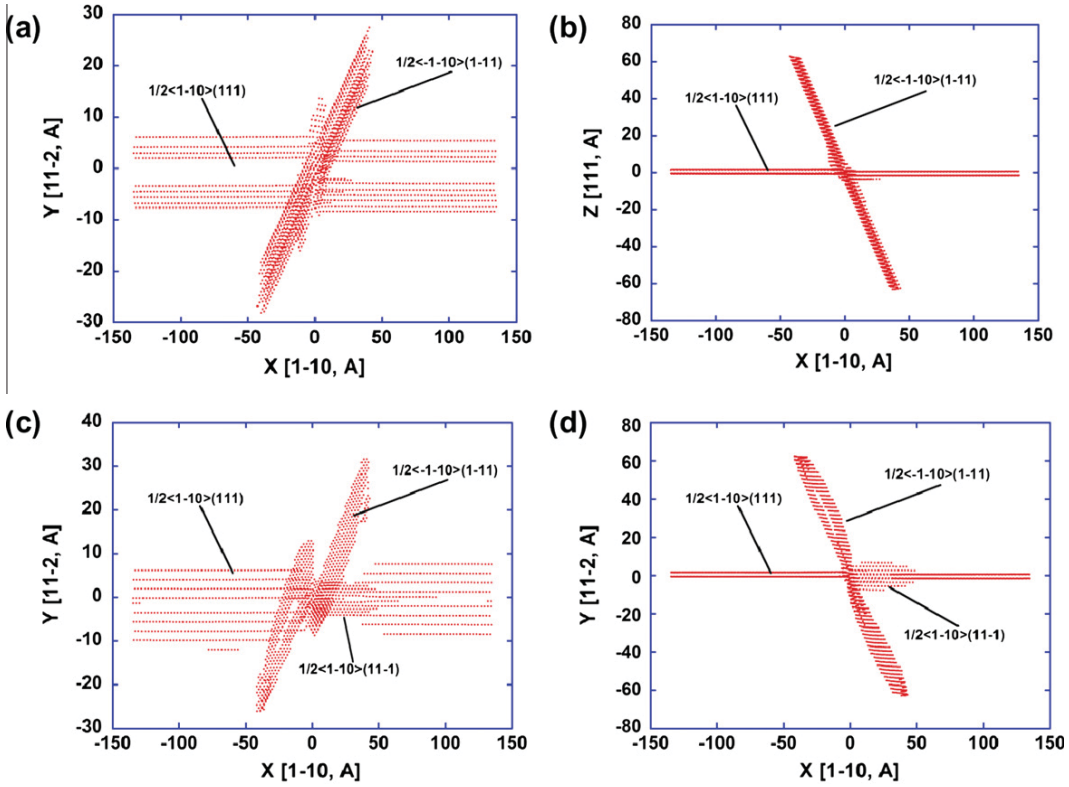

Fig. 10. Initial conditions for the simulation of a fully glide plane structure at a 120° intersection forming a HL with the Ni Mishin potential in (a) the 1 1 1 and (b) the 1 1 $\bar{2}$ projections. The screw dislocation is split into Shockley partials with a separation distance of 4*b* on the (1 1 1) glide plane. (c and d) The relaxed minimum energy structures corresponding to the initial conditions shown in (a and b) in (c) the 1 1 1 and (d) the 1 1 $\bar{2}$ projections. Part of the screw dislocation at the intersection spontaneously spreads on the cross-slip plane.

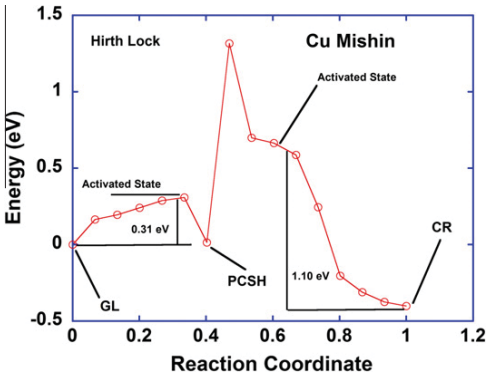

Fig. 11. Energy versus reaction coordinate obtained using the NEB method with the Cu Mishin potential at a 120° screw dislocation intersection forming a HL. The initial separation distance between the screw and intersecting dislocation on the (1 1 1) glide plane was 0. A reaction coordinate of 0 corresponds to the fully glide plane state (GL) and a reaction coordinate of 1 corresponds to the fully cross-slipped state (CR).

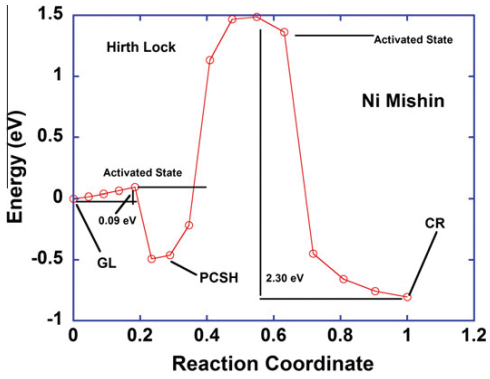

Fig. 12. Energy versus reaction coordinate obtained using the NEB method with the Ni Mishin potential at a 120° screw dislocation intersection forming a HL. The initial separation distance between the screw and intersecting dislocation on the (1 1 1) glide plane was 0. A reaction coordinate of 0 corresponds to the state shown in Fig. 10c and d (GL) and a reaction coordinate of 1 corresponds to the fully cross-slipped state (CR).

dislocation on the (1 1 1) glide plane was varied to find a minimum in this activation energy. The present results are in reasonable accord with previously determined values for the cross-slip activation energy at a 120° intersection using an Escaig stress technique, under selected conditions.

The simulations in this work show that the nucleation of cross-slip at dislocation–dislocation interactions is significantly more probable than that for the FE process, having an activation barrier that is a factor of 3–20 lower. Further, this work shows that atomistic simulations can be used to

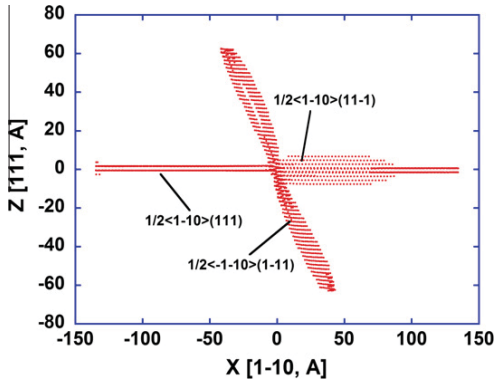

Fig. 13. A plot of the structure of the activated state for transforming the dislocation from the fully glide plane state (GL) to the partially cross-slipped state obtained using the Cu Mishin potential at a 120° intersection forming a HL. The structure is shown in the [1 1 $\bar{2}$] projection. The activated structure was obtained for an initial separation distance of 0 between the screw and intersecting dislocation on the (1 1 1) glide plane.

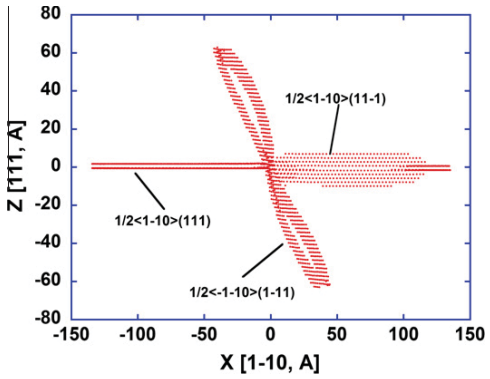

Fig. 14. A plot of the structure of the activated state transforming the dislocation from the state shown in Fig. 10c and d (GL) to the partially cross-slipped state obtained using the Ni Mishin potential at a 120° intersection forming a HL. The structure is shown in the [1 1 $\bar{2}$] projection. The activated structure was obtained for an initial separation distance of 0 between the screw and intersecting dislocation on the (1 1 1) glide plane.

identify types of interactions that result in cross-slip and these results may, in turn, be used in higher level mesoscale simulations.

Summarizing the results.

1. The activation barrier for cross-slip from the fully glide plane state (GL1) to the partially cross-slipped state (PCS1) $\delta E_{\text{GL1-PCS1}}$ at a 120° intersection forming a GL is determined to be a factor of 4 lower than that for the conventional FE-based mechanism in Ni. In Cu it is determined to be a factor of 2.5 lower than that for the conventional FE-based mechanism.
2. The activation barrier for cross-slip from the fully cross-slip plane state (LC2) to the partially cross-slipped state (PCS1) $\delta E_{\text{LC2-PCS1}}$ at a 120° intersection forming a LCL is determined to be approximately a factor of 3 lower than for the FE process in Ni. In Cu it is determined to be approximately a factor of 2.5 lower than FE mechanism cross-slip. These $\delta E_{\text{LC2-PCS1}}$ values are identified, by symmetry, as the activation barrier for cross-slip from the fully glide plane state to the partially cross-slipped state at a 120° screw dislocation intersection, where the intersecting dislocation has a ½⟨0 1 1⟩ Burgers vector, ⟨1 0 $\bar{1}$⟩ line direction and resides on the (1 $\bar{1}$ 1) plane.
3. The activation barrier for cross-slip from the fully glide plane state (GL) to the partially cross-slipped state (PCSH) $\delta E_{\text{GL-PCSH}}$ at a 120° intersection forming a HL is determined to be a factor of 20 lower than that for the conventional FE-based mechanism in Ni. In Cu it is determined to be a factor of 6 lower than that for the conventional FE mechanism. These $\delta E_{\text{GL-PCSH}}$ values are identified, by symmetry, as the activation barrier for cross-slip from the fully cross-slipped state to the partially cross-slipped state at a 120° screw dislocation intersection, where the intersecting dislocation has a ½⟨$\bar{1}$ $\bar{1}$ 0⟩ Burgers vector, ⟨1 0 $\bar{1}$⟩ line direction and resides on the (1 $\bar{1}$ 1) plane.
4. Cross-slip activation energy values near forest dislocation intersections forming GL, LCL and HL in fcc Cu are determined to be 0.65, 0.67 and 0.31 eV. These values are somewhat lower than the experimentally determined value for cross-slip activation energy in Cu (0.61 eV) [12]. This suggests that cross-slip preferentially occurs at selected screw dislocation intersections in fcc materials.

References

[1] Puschl W. Prog Mater Sci 2002;47:415.
[2] Jackson PJ. Prog Mater Sci 1985;29:139.
[3] Rao S, Parthasarathy TA, Woodward C. Philos Mag A 1999;79:1167.
[4] Rao S, Dimiduk DM, El-Awady J, Parthasarathy TA, Uchic MD, Woodward C. Philos Mag 2009;89(34):3351.
[5] Rao S, Dimiduk DM, Jaafar El-Awady, Parthasarathy TA, Uchic MD, Woodward C. Acta Mater 2010;58:5547.
[6] Plimpton SJ. J Comp Phys 1995;117:1.
[7] Henkelman G, Jonsson H. J Chem Phys 2000;113(22):9978.
[8] Rodney D. Phys Rev B 2007;76:144108.
[9] Angelo JE, Moody NR, Baskes MI. Modell Simul Mater Sci Eng 1995;3:289.
[10] Mishin Y. Acta Mater 2004;52:1451.
[11] Mishin Y, Mehl MJ, Papaconstantopoulos DA, Voter AF, Kress JD. Phys Rev B 2001;63:224106.
[12] Couteau O, Kruml T, Martin JL. Acta Mater 2011;59:4207.
[13] Brown LM. Philos Mag A 2002;82:1691.
[14] Vegge T, Jacobsen KW. J Phys Condens Matter 2002;14:2929.
[15] Rao S, Dimiduk DM, Jaafar El-Awady, Parthasarathy TA, Uchic MD, Woodward C, submitted for publication.
[16] Washburn J. Appl Phys Lett 1965;7:183.
[17] Devincre B, Hoc T, Kubin L. Science 2008;320:1745.
[18] Kocks UF, Mecking H. Prog Mater Sci 2003;48(3):102.